



Published in final edited form as:

J Proteomics. 2009 August 20; 72(6): 1046–1060. doi:10.1016/j.jprot.2009.06.011.

Proteome Profile of Functional Mitochondria from Human Skeletal Muscle Using One-Dimensional Gel Electrophoresis and HPLC-ESI-MS/MS

Natalie Lefort^{1,3}, Zhengping Yi^{1,2}, Benjamin Bowen⁴, Brian Glancy³, Eleanna A. De Filippis¹, Rebekka Mapes¹, Hyonson Hwang^{1,3}, Charles R. Flynn¹, Wayne T. Willis³, Anthony Civitarese^{1,3}, Kurt Højlund⁵, and Lawrence J. Mandarino^{1,2,3,*}

¹Center for Metabolic Biology, Arizona State University, Tempe, Arizona

²School of Life Sciences, Arizona State University, Tempe, Arizona

³Department of Kinesiology, Arizona State University, Tempe, Arizona

⁴Harrington Department of Bioengineering, Arizona State University, Tempe, Arizona

⁵Diabetes Research Centre, Department of Endocrinology, Odense University Hospital, Odense, Denmark

Abstract

Mitochondria can be isolated from skeletal muscle in a manner that preserves tightly coupled bioenergetic function *in vitro*. The purpose of this study was to characterize the composition of such preparations using a proteomics approach. Mitochondria isolated from human *vastus lateralis* biopsies were functional as evidenced by their response to carbohydrate and fat-derived fuels. Using one-dimensional gel electrophoresis and HPLC-ESI-MS/MS, 823 unique proteins were detected, and 487 of these were assigned to the mitochondrion, including the newly characterized *SIRT5*, *MitoNEET* and *RDH13*. Proteins detected included 9 of the 13 mitochondrial DNA-encoded proteins and 86 of 104 electron transport chain (ETC) and ETC-related proteins. In addition, 59 of 78 proteins of the 55S mitoribosome, several TIM and TOM proteins and cell death proteins were present. This study presents an efficient method for future qualitative assessments of proteins from functional isolated mitochondria from small samples of healthy and diseased skeletal muscle.

Keywords

HPLC-ESI-MS/MS; human skeletal muscle; mitochondria; one-dimensional-gel electrophoresis; proteome

© 2009 Elsevier B.V. All rights reserved

Address for Correspondence: Lawrence J. Mandarino, Ph.D. Center for Metabolic Biology College of Liberal Arts and Sciences PO Box 873704 Tempe, Arizona 85287-3704, U.S.A. Phone: 1-480-965-8365 FAX: 1-480-727-6183 Email: Lawrence.Mandarino@asu.edu.

Publisher's Disclaimer: This is a PDF file of an unedited manuscript that has been accepted for publication. As a service to our customers we are providing this early version of the manuscript. The manuscript will undergo copyediting, typesetting, and review of the resulting proof before it is published in its final citable form. Please note that during the production process errors may be discovered which could affect the content, and all legal disclaimers that apply to the journal pertain.

Introduction

Amitochondriate cells, such as erythrocytes, are viable, but are highly dependent on glycolysis [1]. The symbiosis of the mitochondrion with the anaerobic eukaryotic cell has provided the host with a number of the organelle's functions, the most important being aerobic metabolism which provides ATP as a source of chemical energy. A proportion of these mitochondrial functions are ubiquitous to all tissues: ion and metabolite transport, fuel oxidation, ATP production, regulation of oxidative stress, heme biosynthesis, cell survival and death [2]. However, tissue-specific functions (urea metabolism in liver, γ -aminobutyric acid metabolism in brain, and dominance of oxidative phosphorylation in heart) of mitochondria correlate with increased expression of proteins that are involved in the upregulated pathway [3-5] although the consequences of post-translational modifications on the activity of mitochondrial proteins cannot be disregarded, particularly OXPHOS subunits, which all can be phosphorylated [6]. The vast majority, about 99%, of mitochondrial proteins are coded by the nuclear genome (13 are coded by mitochondrial DNA (mtDNA)), with estimates for the mammalian mitoproteome ranging from 1000-4200 proteins [7-9], and estimate of the human mitochondrial proteome nearing 1500 proteins [7].

Even though there are considerable challenges in the solubilization of hydrophobic peripheral and integral membrane subunits, which characterizes mitochondrial proteins (ex: electron transport chain (ETC) subunits) [10], interest in the mammalian mitochondrial proteome is flourishing. This stems from an increased acknowledgment of the involvement of this organelle in disease, whereby one or more of its functions are compromised by mutations in mtDNA or nuclear-encoded mitochondrial genes, changes in the metabolic milieu, allosteric regulators and cell signaling. Mitochondrial dysfunction is thought to be implicated in the development and/or progression of neurodegenerative diseases, such as Parkinson's and Alzheimer's disease, cancer, aging, encephalomyopathies and cardiomyopathies (for review see [11]). The role of mitochondrial dysfunction in type 2 diabetes mellitus remains a matter for investigation [12-15]. Several attempts to define the mammalian mitochondrial proteome have proven to be successful [4,5,16-20], although few studies have focused on human tissue [7,21-23], and none on fully functional human mitochondria. To date, the largest human mitochondria proteome description stems from Taylor et al [7] and Gaucher et al [23], whom identified 615 and 680 proteins, respectively, from a single human heart mitochondrial preparation.

Isolation from skeletal muscle of mitochondria that can be used for functional analysis in vitro are useful for studies of mechanisms regulating normal physiology as well as pathophysiological states [13,22,24-29]. The present study was undertaken to characterize the proteome of preparations of highly coupled, fully functional, human skeletal muscle mitochondria. Analysis of functional human skeletal muscle mitochondria by HPLC-ESI-MS/MS identified a total of 823 proteins: 487 known mitochondria proteins (388 assigned by gene ontology (GO) to mitochondria and 99 manually annotated to mitochondria using published experimental evidence) resulting in a list of 336 mitochondria-associated proteins. We demonstrate, for the first time, that both functional and proteomic assessments can be done on metabolically-active mitochondria isolated from a small (100 mg) sample of human skeletal muscle. These data hold promise for global analysis of functional and quantitative changes in the mitochondrial proteome of patients affected by disorders involving skeletal muscle and potentially assist in interpreting functional assays using these mitochondria

Materials and methods

Subjects

A percutaneous needle muscle biopsy was taken under local anesthesia from the *vastus lateralis* muscle of healthy volunteers (males, 40 ± 10 years old (range: 26 to 59), body mass

index: $24 \pm 1 \text{ kg/m}^2$; percent body fat: $21 \pm 2 \%$) with normal glucose tolerance, with no family history of type 2 diabetes and not taking medication known to affect glucose metabolism. The muscle biopsy was taken after the subject had consumed nothing but water overnight, and while the subject rested in a supine position. The subject had been informed to maintain a normal diet and not to engage in vigorous physical activity for 3 days prior to the study. The purpose, nature and potential risks of the study were explained to the participant, and written consent was obtained before participation. The protocol was approved by the Institutional Review Board of Arizona State University.

Small-scale isolation of mitochondria

Following the biopsy, the muscle specimen was trimmed of visible fat, immediately weighed, minced and subjected to a protease (Type XXIV, Sigma Chemical Co., St-Louis, MO) digestion for 7 min. Mitochondria were isolated by a modified method of Makinen and Lee [30] using a protease (Sigma, P-8038) treatment to liberate both subsarcolemmal and intermyofibrillar mitochondria. Briefly, the muscle biopsy (~100 mg) was treated with protease for 7 mins, followed by a glass to glass homogenization using a Con-Torque homogenizer (10 passes). The crude homogenate was centrifuged at $800 \times g$ (10 min, 4°C) to rid the homogenate of cellular debris and nuclei. The supernatant was then centrifuged at $14,000 \times g$ (10 min, 4°C). The pellet, containing the mitochondrial fraction, was resuspended in SOLUTION II (in mM: 100 KCl, 40 Tris-HCl, 10 Tris-Base, 1 MgCl_2 , 0.1 EDTA, 0.2 ATP, 1.5% FFA free BSA, pH 7.5 at 4°C). Following centrifugation at $7,000 \times g$ (10 min, 4°C), the pellet was resuspended in SOLUTION III (in mM: 100 KCl, 40 Tris-HCl, 10 Tris-Base, 1 MgCl_2 , 0.1 EDTA, 0.2 ATP, pH 7.5 at 4°C). A final centrifugation at $3,500 \times g$ (10 min, 4°C) yielded a mitochondrial pellet which minimal endogeneous cytosolic fuel substrates remain. The pellet was resuspended in 100 μl mannitol sucrose buffer (in mM: 220 mannitol, 70 sucrose, 10 Tris-HCl, 1 EGTA) and kept on ice for the duration of the respiration studies.

Immunoblotting

Twenty micrograms of mitochondrial lysate and whole muscle lysate (from the same individual) were resolved by 12.5% SDS-PAGE, transferred to a nitrocellulose membrane and analyzed by western blot. Blot was blocked with 5% non-fat milk in 1X Tris-buffered saline (Bio-Rad, Hercules, CA) and 0.2% Tween 20, incubated with primary antibody overnight at 4°C (in 5% non-fat milk, ATP synthase beta subunit; 1:2500, Molecular Probes, Invitrogen, Carlsbad, CA), and then incubated with a secondary horseradish-conjugated antibody for 1 hr at room temperature (anti-mouse IgG, Santa Cruz, CA). Immunoreactive bands were visualized by enhanced chemiluminescence (Western Lightning Plus, Perkin-Elmer, CT).

Mitochondrial function assessment

To ensure that the mitochondrial preparations were of high quality, mitochondrial coupling, represented by the ADP/O ratio ($\text{ADP/O} = 125 \text{ nmol ADP}/(\text{natom O}_2 \text{ consumed during state 3})$) and the respiratory control ratio ($\text{RCR}, J_{\text{O}_2 \text{ state 3}}/J_{\text{O}_2 \text{ state 4}}$, with 1 mM malate + 1 mM pyruvate, J_{O_2} =oxygen consumption) were assessed. The oxygen electrode was calibrated prior to use using $\text{Na}_2\text{S}_2\text{O}_4$ to establish the zero oxygen line. Since the calibration is performed using ddH_2O , a correction factor for the quantity of dissolved oxygen in the respiration medium relative to ddH_2O was determined. Wanders respiration medium (in mM: 100 KCl, 50 MOPS, 10 K_2HPO_4 , 20 glucose, 10 MgCl_2 , 1 EGTA, 0.2% BSA), at pH=7.0 and 37°C , contained 1.8 times the oxygen content of ddH_2O . To measure respiration, an aliquot of the mitochondria enriched fraction (2.5-10 μl) was placed in a DW1 Electrode Chamber (Hansatech Instruments Ltd, Norfolk, England) which contained 250 μl Wanders respiration medium at 37°C . Using the Oxygraph Plus software provided by Hansatech, carbohydrate- (1 mM malate, 1 mM pyruvate, 10mM glutamate, 5mM succinate) and fatty acid-stimulated (1 mM malate + 10

μ M palmitoyl-DL-carnitine) state 3 (ADP-stimulated, 0.5mM) and state 4 (absence of ADP) respiration rates were measured.

Mitochondria solubilization

Mitochondrial proteins were prepared for proteomic analysis by freeze-thaw homogenization ($3 \times$ liquid N₂ and 37° C) followed by the addition of an equal volume of 2X lysis buffer (1X, in mM: 50 Hepes, 150 NaCl, 0.02 sodium pyrophosphate, 20 beta-glycerophosphate, 10 NaF, 50 SDS, 0.001 NaVO₄, 0.001 phenylmethanesulphonylfluoride (PMSF), 10 μ g/ μ l leupeptin and 10 μ g/ μ l aprotinin). In a study that compared the effectiveness of different detergents in solubilizing integral membrane proteins within the inner mitochondrial membrane (constituting about 50% of inner mitochondrial membrane proteins [31]), 1-10% SDS was as effective as any other combination of detergents [10]. The suspension was incubated on ice for 30 min, followed by a 5 min sonication. Protein concentration of the supernatant was determined using Coomassie Plus Protein Assay Reagent (Bio-Rad, Hercules, CA).

Mass spectrometry sample preparation

Sixty (for subjects 1, 2 and 3) and 240 μ g (subject 1 only) of mitochondrial protein were separated by one dimensional SDS polyacrylamide gel (10%). Two different quantities of soluble mitochondrial protein from subject 1 were loaded in order to test whether 240 μ g maximizes the number of low abundance mitochondrial proteins detected. Proteins were visualized with Coomassie blue (Sigma Chemical Co., St. Louis, MO). Gel lanes were cut into 20 slices of approximately equal size, each slice was destained, dehydrated and digested with trypsin (Sigma Chemical Co., St. Louis, MO) as previously described in detail [32,33]. The volume of the extracted peptide solution was reduced to 5 μ l by vacuum centrifugation, and 20 μ l of 0.05% heptafluorobutyric acid (HFBA)/1% FA/2% acetonitrile (ACN) was added.

Mass spectrometry

HPLC-ESI-MS/MS was performed on a hybrid linear ion trap (LTQ)-Fourier Transform Ion Cyclotron Resonance (FTICR) mass spectrometer (LTQ FT; Thermo Fisher; San Jose, CA) fitted with a PicoView™ nanospray source (New Objective, Woburn, MA). Samples were desalted using an on-line Nanotrap (Michrom Bioresources). On-line capillary HPLC was performed using a Michrom BioResources Paradigm MS4 micro HPLC (Auburn, CA) with a PicoFrit™ column (New Objective). HPLC separations (300nl/min) were accomplished as follows: linear gradient of 2 to 27% ACN in 0.1 % FA in 70 min, hold 5 min at 27% ACN, hold 5 min at 50% ACN and hold 5 min at 80%. A “top-10” data-dependent tandem mass spectrometry approach was utilized to identify peptides in which a full scan spectrum (survey scan) was acquired followed by collision-induced dissociation (CID) mass spectra of the 10 most abundant ions in the survey scan. The survey scan was acquired using the FTICR mass analyzer in order to obtain high resolution, high mass accuracy data.

Data analysis and bioinformatics

Tandem mass spectra were extracted from Xcalibur “RAW” files and charge states were assigned using the Extract_MSN script, a component of Xcalibur 2.0 SR2 (Thermo Fisher; San Jose, CA). Charge states and monoisotopic peak assignments were then verified using DTA-SuperCharge (msquant.sourceforge.net) [5], before all “DTA” files from each gel lane were combined into a single Mascot Generic Format file. The fragment mass spectra were then searched against the IPI_HUMAN_v3.33 database (67 764 entries, <http://www.ebi.ac.uk/IPI/>) using Mascot (Matrix Science, London, UK; version 2.2). The false discovery rate was determined by selecting the option to use a “decoy” randomized search strategy that is available in Mascot v2.2 and was found to be < 1% at the protein level. Search parameters used were: 10 ppm mass tolerance for precursor ion masses and 0.5 Da for product

ion masses; digestion with trypsin; a maximum of two missed tryptic cleavages; variable modifications of oxidation of methionine and phosphorylation of serine, threonine and tyrosine. Probability assessment of peptide assignments and protein identifications were made through use of Scaffold (version 02_00_06, Proteome Software Inc., Portland, OR). Only peptides with $\geq 95\%$ probability were considered. Criteria for protein identification included detection of at least 2 unique identified peptides and a probability score of $\geq 95\%$. Multiple isoforms of a protein were reported only if they were differentiated by at least one unique peptide with $\geq 95\%$ probability, based on Scaffold analysis. UniProt (www.pir.uniprot.org) was used to obtain Gene Ontology annotation (GO). Proteins presenting no mitochondrial GO annotation (GO term: 5739) were manually searched against the Pubmed database (www.ncbi.nlm.nih.gov/PubMed), Gene Cards (www.genecards.org) and Mouse Genome Informatics (www.informatics.jax.org) for evidence of mitochondrial localization.

Results

Relative purity of mitochondria-enriched fraction

Enrichment of mitochondria is demonstrated by the intense signal of the ATP synthase (beta subunit) immunoblot in isolated mitochondria lysate compared to whole muscle lysate (Figure 1A). In addition, ATPase activity, measured by the addition of a bolus of ATP (5mM final) to the isolated mitochondria, was $<4\%$ of the maximal rate generated by Pyr + Mal +ADP. We suspect this value to be even lower with inhibition of ATP synthase (complex V) by oligomycin as used by Bizeau et al [34]. Regardless, this small contamination is in line with Bizeau et al. [34] and others [35, 36] whom deem this an acceptable demonstration of a relatively pure mitochondrial fraction that is suitable for functional assays.

Functional assessment of human skeletal muscle mitochondria

Integrity of the isolated human skeletal muscle mitochondria was evaluated by polarography. A respiratory control ratio of 25 ± 8 (ratio of state 3 to state 4 respiration, RCR), calculated using pyruvate + malate and an ADP/O ratio of 2.3, confirms that the mitochondria were well coupled and fully functional (Figure 1). Measurements of coupling of human skeletal muscle mitochondria range from 2.5-3.0 [13,37,38] for the ADP:O ratio (also referred to as P:O ratio) and values of ~ 12 -14 [13] have been reported for the RCR (using Pyr + Mal). Although our reported ADP:O ratio is 2.3 ± 0.1 , the low state 4 respiration (uncoupled respiration) suggests that the isolation was successful in yielding functional coupled mitochondria. Mitochondria responded to substrate combinations as expected. Maximal concentrations of Glu + Mal, Pyr + Glu + Mal (both complex I-linked fuels) and Pyr + Glu + Mal + Succ (complex I and II-linked fuels; Citric Acid Cycle fully activated) resulted in higher respiration rates than Pyr + Mal (complex I-linked fuel) alone, as reported previously [39,40]. High resting respiration rates (state 4) are observed when mitochondrial structure is compromised and ATP hydrolysis is occurring via ATP synthase released from the damaged mitochondria, providing a continuous pool of ADP to the active mitochondria. In the present study, resting respiration rates were low (Figure 1), indicative of the absence of damaged mitochondria. Citrate synthase (CS) activity from the mitochondrial preparations was $6.9 \pm 0.9 \mu\text{mol min}^{-1} \text{g muscle wet weight}^{-1}$. Assuming a whole muscle CS activity of $12 \mu\text{mol min}^{-1} \text{g muscle wet weight}^{-1}$ in untrained resting human skeletal muscle [41], this implies that about 58 % of the mitochondria were recovered during the isolation, similar to the yield reported in human quadriceps muscle [42].

Proteome of functional human skeletal muscle mitochondria

HPLC-ESI-MS/MS-based analysis of fully functional mitochondria resolved by 1D gel electrophoresis was performed. From the three 60 μg and the single 240 μg fraction, 660, 555, 565 and 690 (average: 618 proteins) unique proteins were identified, respectively. Four-

hundred and forty-six 'core' proteins were found in all three 60 μg mitochondrial fractions (Figure 2A). When combining proteins detected in the four samples, a total of 823 unique proteins were identified after reduction for redundancy. A detailed list of all proteins identified in this study, together with their IPI ID, molecular mass, sequence coverage, and number of unique peptides assigned to each protein are provided as supplemental information (Supplemental Table 1).

Molecular mass and isoelectric point distribution

Molecular mass distribution of all 823 identified proteins is shown in Figure 2C. Proteins ranged from 5.8 kDa (*ATP5E*, ATP synthase epsilon chain) to 3,800 kDa (*TTN*, Titin). Upon comparison of the molecular mass distribution of the proteins detected in the mitochondrial preparation *versus* those detected in the human skeletal muscle proteome [43], it is clear that a greater number of lower molecular mass (<40 kDa) proteins were detected in the mitochondrial fraction ($64 \pm 0.8\%$ in mitochondria *vs.* 42% in whole muscle). The higher fraction of lower molecular mass proteins in the mitochondrial preparation is suggestive of a higher abundance of lower molecular mass proteins within this organelle compared to whole muscle proteins. In order to confirm that the sample preparation was not selective of non-membrane proteins, we compared the isoelectric point (pI) values for the detected *vs.* the non-detected subunits of the ETC. The calculated pI allows for the estimation of the subcellular localization of proteins, with membrane bound proteins averaging a pI value of approximately 8.5 to 9 [44]. The theoretical pI of the individual ETC subunits was determined (http://ca.expasy.org/tools/pi_tool.html). Eighty-two percent of the 55 detected ETC subunits have a pI over 8.5 and 64% over 9. Sixty-three percent of the 16 undetected subunits have a calculated pI of 8.5 and 50% over 9, suggesting that the lack of detection of certain ETC subunits was not due to the non-solubilization of integral membrane proteins. Solubilization of the mitochondria using the approach described above was efficient, and most integral membranal proteins were released from their phospholipid environment. Furthermore, increasing protein loading to maximize the number of unique mitochondrial proteins detected was successful.

Gene Ontology Distribution

Using solely cellular location information as assigned by GO annotations, we identified 388 (range: 301-336) unique mitochondrial proteins (GO term: 5739) from isolated mitochondria, while only 212 unique mitochondrial proteins (range: 117-144) were assigned by this GO term in the whole muscle homogenates [32]. Of 563 proteins for which Gene Ontology (GO) information were available (Figure 3A), 388 (69%) proteins were assigned to mitochondria. Fewer proteins of nuclear, cytoskeletal and extracellular origin were detected in the mitochondrial preparation as compared to the human skeletal muscle proteome [43] (Figure 3B). The distribution of the GO-annotated mitochondrial proteins among different mitochondrial processes are given in Figure 3C. Several uncharacterized and newly characterized proteins with evidence of mitochondrial localization were detected (Table 1). When the spectra of the 99 proteins localized to mitochondria by previously published experimental evidence (see Methods for details and Suppl. Table 2) are considered along with the 388 GO-annotated mitochondrial proteins, $59 \pm 4\%$ (range: 52-71 %) of the spectra originate from mitochondrial proteins. Only 8 % of the total spectra belonged to mitochondrial proteins in the whole muscle dataset recently reported by our laboratory under the same MS conditions [43], suggesting that the mitochondrial isolation procedure successfully enriches mitochondrial proteins by ~7-fold. In light of this, we compared the dataset generated by a whole muscle proteome analysis (60-75 μg per subject, n=3 healthy lean subjects) [43] and the present mitoproteome (60 μg lane, n=3 healthy lean subjects). Using fraction of spectra, which has been shown to be an effective method for quantitative proteomics research [45-48], we estimated the relative abundance of specific proteins within these samples. All proteins in the

CAC and FA oxidation pathways detected in the mitochondrial preparation had a higher fraction of spectra (CAC, 20 proteins detected: 6.0 ± 0.7 and FA oxidation pathway, 18 proteins detected: 8.9 ± 1.6 fold increase) in the current analysis than in the whole muscle proteome, indicative of their enrichment. Twenty-three \pm three (range: 13-28 %) percent of the spectra from the mitoproteome were generated by myosin isoforms (myosin-2 and -7, myosin light chains and myosin binding protein). Myosin isoforms are the major component of skeletal muscle proteins and it is extremely difficult to separate all of these from mitochondria, especially in isolation conditions where the function of the organelle is preserved. The remaining 19 % of spectra were generated from 326 (10 myosin-related proteins not included) mitochondria-associated proteins, of which 14 (Supplemental Table 1) are predicted to be mitochondrial by MitoPRED (<http://bioinformatics.albany.edu/~mitopred>) [49,50] and 43 have yet to be assigned a cellular localization (Table 1).

Mitochondrial and nuclear DNA-encoded proteins

Detection of mtDNA-encoded proteins by mass spectrometry has posed some challenges and has required some technical adaptations in previous characterizations of the mitochondrial proteome [7,51]. Using a simple detergent-based method, from 420 μ g mitochondrial protein, we have successfully detected 9 of the 13 polypeptides encoded by mtDNA (Figure 4). Of the 823 unique proteins detected, 814 are nuclear-encoded proteins.

Electron transport

The electron transport chain is comprised of 104 members distributed among the 5 ETC complexes (subunits from complexes I-V), the ubiquinone complex (ubiquinone biosynthesis proteins), the electron transfer flavoprotein complex and cytochrome c. The ADP/ATP translocases and the phosphate carriers complete the oxidative phosphorylation machinery, and are discussed further in the following section. For complex I (NADH:ubiquinone oxidoreductase), II (succinate dehydrogenase: ubiquinone oxidoreductase), III (ubiquinol:cytochrome c oxidoreductase), IV (cytochrome c oxidase) and V (ATP synthase), 38, 3, 7, 12 and 16 subunits were detected, respectively. Furthermore, *C6ORF66*, an assembly factor of complex I, was detected. Figure 5 lists the individual subunits in each complex which were identified.

Citric acid cycle (CAC) and fatty acid oxidation

Subunits from the pyruvate dehydrogenase complex, which funnels acetyl-CoA into the CAC and the 8 key enzymes of the CAC (subunit d from succinate dehydrogenase undetected) were detected (Figure 6A). Furthermore, we identified all major enzymes of the FA oxidation pathway (Figure 6B).

Mitochondrial import of proteins and substrates

Key transporters in substrate shuttling between the mitochondrial matrix, intermembrane space and the cytoplasm were identified, including phosphate carrier protein, ADP/ATP translocases (*SLC25A4/5/6*), carnitine O-palmitoyltransferase $\frac{1}{2}$ (*CPT1B/2*), and the voltage-dependent anion channels $\frac{1}{2/3}$ (*VDAC1/2/3*). Additionally, Arl2 GTPase (*ARL2*), which exists in cytosolic and mitochondrial pools, was detected. Arl2 GTPase in a complex with its binding partner, binder of Arl2 (*BART*), and GTP enter the mitochondria and bind to the adenine nucleotide translocator (*SLC25A4/5/6*) [52]. Since 99% of mitochondrial proteins are synthesized within the cytoplasm, mitochondria have developed a complex network of proteins called TOM, TIM and SAM proteins involved in the transport of nuclear-encoded mitochondrial protein precursors into their respective mitochondrial compartments (for review see [53]). A list of TOM, TIM and SAM proteins identified in the present study are given in Table 2 under the section 'Import Machinery and Transporters'. Once the import of matrix

proteins complete, the mitochondrial localization signal is cleaved by specific peptidases, such as mitochondrial-processing peptidase alpha and beta subunits (see Table 2)

Nucleoproteins

Mitochondrial DNA segregates into discrete DNA-protein complexes, of which the DNA-binding proteins [47] involved and detected in the present dataset include proteins involved in DNA replication (ex: *TFAM* [54], *SSBP1* [47]), transcription (ex: *PTRF* [55]), segregation during fusion and fission events and maintenance [55]. Interestingly, *PHB1/2* [56], *HSPD1/A9*, *ATAD3A*, *HADHA* and *LRPPRC* [47] have been localized to nucleoid-like complexes and were detected in the present dataset.

Protein synthesis

Mitochondrial DNA codes for 2rRNAs and 22 tRNA synthetases. The 55S mammalian mitoribosome is protein-rich, with a protein abundance about 2-fold that of prokaryotic mitochondrial ribosomes [57]. In the present analysis, 25 of the 31 (81%) mitochondrial ribosomal proteins which are contained within the 28S small ribosomal subunit (MRPSs), and 34 of the 48 (71%) MRPLs found in the 39S large subunit [58] were detected. Three isoforms of *MRPS18* exist and may play a role in the localization of the mitoribosome within the mitochondria [59]. Two isoforms of *MRSP18* (A and B) were detected.

Amino acid catabolism

Branched chain amino acids have gained interest as they are activators of mTOR [60], which is involved in the pathogenesis of insulin resistance [61,62] and is a novel player in mitochondrial biogenesis [63]. We detected all 3 components of the branched chain alpha keto acid dehydrogenase complex: 2-oxoisovalerate dehydrogenase alpha subunit (E1), lipoamide acyltransferase (E2) and alpha-ketoglutarate dehydrogenase (E3). Leucine (methylcrotonoyl-CoA carboxylase, hydroxymethylglutaryl-CoA lyase and isovaleryl-CoA dehydrogenase) and glycine (glycine cleavage system H protein) catabolic enzymes were detected. Glutaryl-CoA dehydrogenase was detected, a degradative enzyme involved in L-lysine, L-hydroxylysine, and L-tryptophan oxidation (refer to Table 2).

Oxidative stress proteins

Mitochondria are key contributors to reactive oxygen species (ROS) generation. At lower concentrations, ROS are important modulators of signaling cascades (e.g. glucose transport) [64], however at higher concentrations, ROS are detrimental to DNA integrity and protein function, ultimately leading to cell death [65,66]. Proteins implicated in ROS generation and scavenging can be found in Table 2, under 'Oxidative Stress Proteins'. The accumulation of oxidative damage is thought to be the key contributor to cellular aging [67] and cell death [68]. Mitochondria initiate cell death via the release of pro-apoptotic mitochondrial proteins via the mitochondrial permeability transition pore. Pro- and anti-apoptotic proteins detected are listed in Table 2 under 'Cell death-related protein'.

Comparison with human skeletal muscle gene expression

The present human skeletal muscle mitochondrial proteome was compared to a gene expression dataset compiled from human skeletal muscle from lean healthy subjects (n=6). Eighty-eight percent of the proteins detected in isolated mitochondria had detectable levels of their respective mRNA at the level of whole muscle. The observation that 12% of detected proteins in isolated mitochondria had undetectable levels of mRNA transcripts in whole muscle is in agreement with previously published data from our laboratory [33], where 59 of the 507 (12 %) proteins detected in muscle biopsies from 4 out of 6 subjects were called absent in the mRNA analysis.

Detection of phosphorylation sites

Although no attempt was made to enrich phosphopeptides, 19 phosphorylation sites in fifteen proteins were detected with confidence (95% using Scaffold analysis (Supplemental Table 3). Of the 19 phosphorylation sites identified, 10 were from known mitochondrial proteins, including cytochrome c, aspartate aminotransferase, ADP/ATP translocase 1, voltage-dependent anion channel 1/2 and creatine kinase type M.

Discussion

The purpose of the present study was to characterize the proteome of preparations of mitochondria isolated from human skeletal muscle in a manner that provides fully functional organelles. This study represents the first proteomic profile of such functional mitochondria. Our proteomic analysis of isolated functional human skeletal muscle mitochondria, using one-dimensional gel electrophoresis followed by HPLC-ESI-MS/MS, assigned 823 proteins. Of these, 388 could be characterized as mitochondrial proteins using GO annotations, while an additional 99 proteins were identified as mitochondrial in origin, using other databases, for a total of 487 (59 % of proteins detected) mitochondrial proteins. Of the remaining 336 proteins that were assigned in this preparation, 14 were predicted to be of mitochondrial origin by MITOPRED [49,50] and 43 were of undefined subcellular localization. Currently, this is the most comprehensive list of proteins of functional mitochondria from human skeletal muscle. The largest dataset of the human skeletal muscle mitochondrial proteome previously generated was compiled indirectly and yielded 212 mitochondrial proteins from the human skeletal muscle proteome dataset [43]. In the present study, 59 % of the spectra generated were assigned to the 487 mitochondrial proteins, whereas 8% of the spectra belonged to the 212 mitochondrial proteins in the whole muscle dataset [43]. This study demonstrates that a greater than 7-fold enrichment of mitochondrial proteins is possible using a procedure for isolation of muscle mitochondria which has been widely used for measurement of mitochondrial respiration in rodent muscle [24-28] and small clinical samples from human individuals [13,29,69].

Of the 487 mitochondrial proteins that were detected in isolated mitochondria in the present study, 232 were not detected in whole muscle homogenates, using the same mass spectrometry conditions [43]. Of these 232 proteins, specific subsets of proteins were enriched, including: pyruvate dehydrogenase-related proteins, mitochondrial protein importers, iron-related proteins, several tRNA synthetases, and enzymes involved in the degradation of amino acids, in particular branched-chain amino acids. Importantly, only one 28S and one 39S ribosomal protein were detected in the muscle proteome [43] versus 59 mitochondrial ribosomal proteins (MRPs) detected in this study. The identification of proteins in mammalian mitochondrial ribosomes has been proved to be a difficult task due to their low copy number [33]. These observations highlight the advantage of employing a mitochondria-enriched preparation for studies focusing on mitochondrial function or biogenesis combined with proteomic analysis.

Our current analysis revealed 99 proteins which were not annotated to mitochondria by GO using the Uniprot search engine, but for which there is experimental evidence linking them to mitochondria (Supplemental Table 2, see Manual Annotation + *GFP proteins in MitoCarta column). Included in this group of proteins is a *MitoNEET* homolog, Zinc finger CDGSH-type domain (*CISD2*). Recently characterized, *MitoNEET* is involved in the regulation of oxidative capacity [70] and is a target of pioglitazone [71]. Also of interest in this group is the detection of *SIRT5*, a lifespan-regulating protein [72], and uncharacterized DNAJ homolog subfamily C member 11 (*DNAJC11*), which was recently found within a human heart mitochondrial immunocomplex consisting of Mitofilin (*IMMT*), sorting and assembly machinery component 50 (*SAMM50*), metaxins 1/2 (*MTX1/2*) and coiled-coil-helix coiled-coil-helix domain-containing protein 3/6 (*CHCHD3*) [73]. Interestingly, *SAMM50*, both *MTX1* and *MTX2* as well as *CHCHD3* were detected in the present mitoproteome. Fourteen proteins among the non-

mitochondrially annotated proteins were predicted to be localized to mitochondria according to MitoPred [49, 50] including coiled-coil-helix coiled-coil-helix domain-containing protein (*CHCHD2/9*), transmembrane protein 109 (*TMEM109*), apolipoprotein O 1/2 (*APOO*), and several open reading frames. More elaborate studies will be required to assess the validity of these predictions.

To our knowledge, we are the first group to report the detection of mtDNA-encoded proteins in human skeletal muscle mitochondria by one-dimensional gel electrophoresis and HPLC-ESI-MS/MS using mitochondrial protein amounts in the ~400 µg range. The use of organic solvents on purified bovine mitochondrial membranes [51] lead to the detection of 10 of the 13 mtDNA-encoded proteins. Taylor and Ghosh [7] detected 9 mtDNA-encoded proteins from 40 mg of purified human heart mitochondria. We detected 9 mtDNA-encoded proteins in the current study without making any special attempt to do so, and using only 420 µg of mitochondria-enriched preparation. Interestingly, three of the four subunits (*ND3*, *ND4L* and *COX3*) absent in this study were not present in the dataset published by Taylor and Ghosh [7].

Previous studies have successfully detected and identified over 600 proteins in isolated mitochondria from rat and human tissues [5,7,23]. However, several hearts and all leg muscles of rats [5] or an entire human ventricle [22] were employed to yield over 10 mg of starting purified mitochondrial material. This is ~25-fold greater than the amount of material used in the present study. The extensive organellar purification steps and methods described in these studies are useful for the detection of novel mitochondrial proteins, but are not practical for proteomic assessments of healthy *versus* pathological states owing to the small tissue sample size that needs to be obtained for use in such studies. However, new potential yet unconfirmed mitochondrial proteins can be extrapolated from a three way comparison of the present and the published existing datasets. We compared the present dataset to both MitoCarta (mitochondria proteome from 14 murine tissues, 1023 human homologs) and the mitochondria proteome from human heart (MitoP2, 618 proteins). Three-hundred and seventeen proteins were common in the three analyses, whereas 216 proteins of the present dataset were found in neither MitoCarta nor the human heart mitochondria proteome (Figure 2b). Pagliarini et al. [20] confirmed the localization of 131 newly-predicted mitochondria-associated proteins by GFP-tagging followed by microscopy. The present study supports this observation for 39 of these 131 proteins (Supplemental Table 2). Of these 39 proteins, thirty are not presently classified as mitochondrial proteins by Gene Ontology. In addition, 8 of the 19 Complex I-associated proteins determined using phylogenetic profiling [20] were confidently identified (*c8orf38*, *c3orf60*, *NDUFS3*, *OXCT1*, *DCI*, *MCCC2*, *LYRM5*, *LACTB*).

In conclusion, this study represents the first application of 1D-gel electrophoresis and HPLC-ESI-MS/MS for analysis of functional human skeletal muscle mitochondria. Using only 420 µg of total mitochondria enriched protein from 3 lean subjects (100 mg muscle biopsy/subject) in 80 HPLC-ESI-MS/MS runs, we provide the most comprehensive coverage of the human skeletal muscle mitochondrial proteome to date. These data demonstrate the utility of this relatively simple proteomic approach for analysis of isolated mitochondria from small human tissue samples, making it a potentially valuable tool in elucidating changes in mitochondrial function and in the mitoproteome associated with human disease.

Supplementary Material

Refer to Web version on PubMed Central for supplementary material.

Acknowledgments

We would like to acknowledge the expert nursing assistance of Julie Roberts and Alexandra Meyer, and technical assistance of Kenneth Kirschner. This study was supported by NIH grants R01DK47936 and R01DK66487 (LJM).

Abbreviations

FA, Formic acid; OXPHOS, oxidative phosphorylation; GO, Gene Ontology annotation; FFA, free fatty acid; TIM, inner membrane translocase; TOM, outer membrane translocase; MRP, mitochondrial ribosomal protein.

References

- [1]. Hyun DH, Hunt ND, Emerson SS, Hernandez JO, Mattson MP, de Cabo R. Up-regulation of plasma membrane-associated redox activities in neuronal cells lacking functional mitochondria. *J Neurochem* 2007;100:1364–74. [PubMed: 17250676]
- [2]. Da Cruz S, Parone PA, Martinou JC. Building the mitochondrial proteome. *Expert Rev Proteomics* 2005;2:541–51. [PubMed: 16097887]
- [3]. Johnson DT, Harris RA, Blair PV, Balaban RS. Functional consequences of mitochondrial proteome heterogeneity. *Am J Physiol Cell Physiol* 2007;292:C698–707. [PubMed: 16971502]
- [4]. Johnson DT, Harris RA, French S, Blair PV, You J, Bemis KG, Wang M, Balaban RS. Tissue heterogeneity of the mammalian mitochondrial proteome. *Am J Physiol Cell Physiol* 2007;292:C689–97. [PubMed: 16928776]
- [5]. Forner F, Foster LJ, Campanaro S, Valle G, Mann M. Quantitative proteomic comparison of rat mitochondria from muscle, heart, and liver. *Mol Cell Proteomics* 2006;5:608–19. [PubMed: 16415296]
- [6]. Huttemann M, Lee I, Samavati L, Yu H, Doan JW. Regulation of mitochondrial oxidative phosphorylation through cell signaling. *Biochim. Biophys. Acta* 2007;1773:1701–20. [PubMed: 18240421]
- [7]. Taylor SW, Fahy E, Zhang B, Glenn GM, Warnock DE, Wiley S, Murphy AN, Gaucher SP, Capaldi RA, Gibson BW, Ghosh SS. Characterization of the human heart mitochondrial proteome. *Nat. Biotechnol* 2003;21:281–6. [PubMed: 12592411]
- [8]. Richly E, Chinnery PF, Leister D. Evolutionary diversification of mitochondrial proteomes: implications for human disease. *Trends Genet* 2003;19:356–62. [PubMed: 12850438]
- [9]. Taylor SW, Fahy E, Ghosh SS. Global organellar proteomics. *Trends Biotechnol* 2003;21:82–8. [PubMed: 12573857]
- [10]. Everberg H, Leiding T, Schioth A, Tjerneld F, Gustavsson N. Efficient and non-denaturing membrane solubilization combined with enrichment of membrane protein complexes by detergent/polymer aqueous two-phase partitioning for proteome analysis. *J. Chromatogr. A* 2006;1122:35–46. [PubMed: 16682048]
- [11]. Reichert AS, Neupert W. Mitochondriomics or what makes us breathe. *Trends Genet* 2004;20:555–62. [PubMed: 15475115]
- [12]. Szendroedi J, Schmid AI, Chmelik M, Toth C, Brehm A, Krssak M, Nowotny P, Wolzt M, Waldhausl W, Roden M. Muscle mitochondrial ATP synthesis and glucose transport/phosphorylation in type 2 diabetes. *PLoS Med* 2007;4:e154. [PubMed: 17472434]
- [13]. Mogensen M, Sahlin K, Fernstrom M, Glintborg D, Vind BF, Beck-Nielsen H, Hojlund K. Mitochondrial respiration is decreased in skeletal muscle of patients with type 2 diabetes. *Diabetes* 2007;56:1592–9. [PubMed: 17351150]
- [14]. Boushel R, Gnaiger E, Schjerling P, Skovbro M, Kraunsøe R, Dela F. Patients with type 2 diabetes have normal mitochondrial function in skeletal muscle. *Diabetologia* 2007;50:790–6. [PubMed: 17334651]
- [15]. Phielix E, Schrauwen-Hinderling VB, Mensink M, Lenaers E, Meex R, Hoeks J, Kooi ME, Moonen-Kornips E, Sels JP, Hesselink MK, Schrauwen P. Lower intrinsic ADP-stimulated mitochondrial

respiration underlies in vivo mitochondrial dysfunction in muscle of male type 2 diabetic patients. *Diabetes* 2008;57:2943–9. [PubMed: 18678616]

- [16]. Lopez MF, Kristal BS, Chernokalskaya E, Lazarev A, Shestopalov AI, Bogdanova A, Robinson M. High-throughput profiling of the mitochondrial proteome using affinity fractionation and automation. *Electrophoresis* 2000;21:3427–40. [PubMed: 11079563]
- [17]. Hanson BJ, Schulenberg B, Patton WF, Capaldi RA. A novel subfractionation approach for mitochondrial proteins: a three-dimensional mitochondrial proteome map. *Electrophoresis* 2001;22:950–9. [PubMed: 11332763]
- [18]. Fountoulakis M, Berndt P, Langen H, Suter L. The rat liver mitochondrial proteins. *Electrophoresis* 2002;23:311–28. [PubMed: 11840540]
- [19]. Da Cruz S, Xenarios I, Langridge J, Vilbois F, Parone PA, Martinou JC. Proteomic analysis of the mouse liver mitochondrial inner membrane. *J. Biol. Chem* 2003;278:41566–71. [PubMed: 12865426]
- [20]. Pagliarini DJ, Calvo SE, Chang B, Sheth SA, Vafai SB, Ong SE, Walford GA, Sugiana C, Boneh A, Chen WK, Hill DE, Vidal M, Evans JG, Thorburn DR, Carr SA, Mootha VK. A mitochondrial protein compendium elucidates complex I disease biology. *Cell* 2008;134:112–23. [PubMed: 18614015]
- [21]. Rabilloud T, Kieffer S, Procaccio V, Louwagie M, Courchesne PL, Patterson SD, Martinez P, Garin J, Lunardi J. Two-dimensional electrophoresis of human placental mitochondria and protein identification by mass spectrometry: toward a human mitochondrial proteome. *Electrophoresis* 1998;19:1006–14. [PubMed: 9638947]
- [22]. Taylor SW, Warnock DE, Glenn GM, Zhang B, Fahy E, Gaucher SP, Capaldi RA, Gibson BW, Ghosh SS. An alternative strategy to determine the mitochondrial proteome using sucrose gradient fractionation and 1D PAGE on highly purified human heart mitochondria. *J Proteome Res* 2002;1:451–8. [PubMed: 12645917]
- [23]. Gaucher SP, Taylor SW, Fahy E, Zhang B, Warnock DE, Ghosh SS, Gibson BW. Expanded coverage of the human heart mitochondrial proteome using multidimensional liquid chromatography coupled with tandem mass spectrometry. *J Proteome Res* 2004;3:495–505. [PubMed: 15253431]
- [24]. Jackman MR, Willis WT. Characteristics of mitochondria isolated from type I and type IIb skeletal muscle. *Am. J. Physiol* 1996;270:C673–8. [PubMed: 8779934]
- [25]. Yajid F, Mercier JG, Mercier BM, Dubouchaud H, Prefaut C. Effects of 4 wk of hindlimb suspension on skeletal muscle mitochondrial respiration in rats. *J. Appl. Physiol* 1998;84:479–85. [PubMed: 9475856]
- [26]. Milner DJ, Mavroidis M, Weisleder N, Capetanaki Y. Desmin cytoskeleton linked to muscle mitochondrial distribution and respiratory function. *J. Cell Biol* 2000;150:1283–98. [PubMed: 10995435]
- [27]. Johnson G, Roussel D, Dumas JF, Douay O, Malthiery Y, Simard G, Ritz P. Influence of intensity of food restriction on skeletal muscle mitochondrial energy metabolism in rats. *Am J Physiol Endocrinol Metab* 2006;291:E460–7. [PubMed: 16621897]
- [28]. Kerner J, Turkaly PJ, Minkler PE, Hoppel CL. Aging skeletal muscle mitochondria in the rat: decreased uncoupling protein-3 content. *Am J Physiol Endocrinol Metab* 2001;281:E1054–62. [PubMed: 11595663]
- [29]. Jackman MR, Ravussin E, Rowe MJ, Pratley R, Milner MR, Willis WT. Effect of a Polymorphism in the ND1 Mitochondrial Gene on Human Skeletal Muscle Mitochondrial Function. *Obesity (Silver Spring)* 2008;16:363–8. [PubMed: 18239645]
- [30]. Makinen MW, Lee CP. Biochemical studies of skeletal muscle mitochondria. I. Microanalysis of cytochrome content, oxidative and phosphorylative activities of mammalian skeletal muscle mitochondria. *Arch. Biochem. Biophys* 1968;126:75–82. [PubMed: 4970348]
- [31]. Nicholls, DGaF; S.J.. *Bioenergetics*. Vol. 3rd ed.. Vol. 3. Academic Press; 2002.
- [32]. Hojlund K, Yi Z, Hwang H, Bowen B, Lefort N, Flynn CR, Langlais P, Weintraub ST, Mandarino LJ. Characterization of the human skeletal muscle proteome by one-dimensional gel electrophoresis and HPLC-ESI-MS/MS. *Mol Cell Proteomics* 2008;7:257–67. [PubMed: 17911086]

- [33]. Yi Z, Bowen BP, Hwang H, Jenkinson CP, Coletta DK, Lefort N, Bajaj M, Kashyap S, Berria R, De Filippis EA, Mandarino LJ. Global relationship between the proteome and transcriptome of human skeletal muscle. *J Proteome Res* 2008;7:3230–41. [PubMed: 18613714]
- [34]. Bizeau ME, Willis WT, Hazel JR. Differential responses to endurance training in subsarcolemmal and intermyofibrillar mitochondria. *J. Appl. Physiol* 1998;85:1279–84. [PubMed: 9760317]
- [35]. Krieger DA, Tate CA, McMillin-Wood J, Booth FW. Populations of rat skeletal muscle mitochondria after exercise and immobilization. *J. Appl. Physiol* 1980;48:23–8. [PubMed: 6444398]
- [36]. Cogswell AM, Stevens RJ, Hood DA. Properties of skeletal muscle mitochondria isolated from subsarcolemmal and intermyofibrillar regions. *Am. J. Physiol* 1993;264:C383–9. [PubMed: 8383431]
- [37]. Fernstrom M, Bakkman L, Tonkonogi M, Shabalina IG, Rozhdestvenskaya Z, Mattsson CM, Enqvist JK, Ekblom B, Sahlin K. Reduced efficiency, but increased fat oxidation, in mitochondria from human skeletal muscle after 24-h ultraendurance exercise. *J. Appl. Physiol* 2007;102:1844–9. [PubMed: 17234801]
- [38]. Bakkman L, Sahlin K, Holmberg HC, Tonkonogi M. Quantitative and qualitative adaptation of human skeletal muscle mitochondria to hypoxic compared with normoxic training at the same relative work rate. *Acta Physiol (Oxf)* 2007;190:243–51. [PubMed: 17521315]
- [39]. Rasmussen UF, Rasmussen HN. Human quadriceps muscle mitochondria: a functional characterization. *Mol. Cell. Biochem* 2000;208:37–44. [PubMed: 10939626]
- [40]. Winkler-Stuck K, Kirches E, Mawrin C, Dietzmann K, Lins H, Wallesch CW, Kunz WS, Wiedemann FR. Re-evaluation of the dysfunction of mitochondrial respiratory chain in skeletal muscle of patients with Parkinson's disease. *J. Neural Transm* 2005;112:499–518. [PubMed: 15340872]
- [41]. Leek BT, Mudaliar SR, Henry R, Mathieu-Costello O, Richardson RS. Effect of acute exercise on citrate synthase activity in untrained and trained human skeletal muscle. *Am J Physiol Regul Integr Comp Physiol* 2001;280:R441–7. [PubMed: 11208573]
- [42]. Rasmussen UF, Rasmussen HN. Human skeletal muscle mitochondrial capacity. *Acta Physiol. Scand* 2000;168:473–80. [PubMed: 10759584]
- [43]. Hojlund K, Yi Z, Hwang H, Bowen B, Lefort N, Flynn CR, Langlais P, Weintraub ST, Mandarino LJ. Characterization of the human skeletal muscle proteome by one-dimensional Gel electrophoresis and HPLC-ESI-MS/MS. *Mol Cell Proteomics*. 2007In press
- [44]. Schwartz R, Ting CS, King J. Whole proteome pI values correlate with subcellular localizations of proteins for organisms within the three domains of life. *Genome Res* 2001;11:703–9. [PubMed: 11337469]
- [45]. Paoletti AC, Parmely TJ, Tomomori-Sato C, Sato S, Zhu D, Conaway RC, Conaway JW, Florens L, Washburn MP. Quantitative proteomic analysis of distinct mammalian Mediator complexes using normalized spectral abundance factors. *Proc Natl Acad Sci U S A* 2006;103:18928–33. [PubMed: 17138671]
- [46]. Liu H, Sadygov RG, Yates JR 3rd. A model for random sampling and estimation of relative protein abundance in shotgun proteomics. *Analytical chemistry* 2004;76:4193–201. [PubMed: 15253663]
- [47]. Wang Y, Bogenhagen DF. Human mitochondrial DNA nucleoids are linked to protein folding machinery and metabolic enzymes at the mitochondrial inner membrane. *J Biol Chem* 2006;281:25791–802. [PubMed: 16825194]
- [48]. Zybailov B, Mosley AL, Sardi ME, Coleman MK, Florens L, Washburn MP. Statistical analysis of membrane proteome expression changes in *Saccharomyces cerevisiae*. *J Proteome Res* 2006;5:2339–47. [PubMed: 16944946]
- [49]. Guda C, Fahy E, Subramaniam S. MITOPRED: a genome-scale method for prediction of nucleus-encoded mitochondrial proteins. *Bioinformatics* 2004;20:1785–94. [PubMed: 15037509]
- [50]. Guda C, Guda P, Fahy E, Subramaniam S. MITOPRED: a web server for the prediction of mitochondrial proteins. *Nucleic Acids Res* 2004;32:W372–4. [PubMed: 15215413]
- [51]. Carroll J, Altman MC, Fearnley IM, Walker JE. Identification of membrane proteins by tandem mass spectrometry of protein ions. *Proc. Natl. Acad. Sci. U. S. A* 2007;104:14330–5. [PubMed: 17720804]

- [52]. Sharer JD, Shern JF, Van Valkenburgh H, Wallace DC, Kahn RA. ARL2 and BART enter mitochondria and bind the adenine nucleotide transporter. *Mol. Biol. Cell* 2002;13:71–83. [PubMed: 11809823]
- [53]. Pfanner N, Wiedemann N, Meisinger C, Lithgow T. Assembling the mitochondrial outer membrane. *Nat Struct Mol Biol* 2004;11:1044–8. [PubMed: 15523480]
- [54]. Alam TI, Kanki T, Muta T, Ukaji K, Abe Y, Nakayama H, Takio K, Hamasaki N, Kang D. Human mitochondrial DNA is packaged with TFAM. *Nucleic Acids Res* 2003;31:1640–5. [PubMed: 12626705]
- [55]. Holt IJ, He J, Mao CC, Boyd-Kirkup JD, Martinsson P, Sembongi H, Reyes A, Spelbrink JN. Mammalian mitochondrial nucleoids: organizing an independently minded genome. *Mitochondrion* 2007;7:311–21. [PubMed: 17698423]
- [56]. Bogenhagen DF, Wang Y, Shen EL, Kobayashi R. Protein components of mitochondrial DNA nucleoids in higher eukaryotes. *Mol Cell Proteomics* 2003;2:1205–16. [PubMed: 14514796]
- [57]. Sharma MR, Koc EC, Datta PP, Booth TM, Spremulli LL, Agrawal RK. Structure of the mammalian mitochondrial ribosome reveals an expanded functional role for its component proteins. *Cell* 2003;115:97–108. [PubMed: 14532006]
- [58]. Zhang Z, Gerstein M. Identification and characterization of over 100 mitochondrial ribosomal protein pseudogenes in the human genome. *Genomics* 2003;81:468–80. [PubMed: 12706105]
- [59]. O'Brien TW, O'Brien BJ, Norman RA. Nuclear MRP genes and mitochondrial disease. *Gene* 2005;354:147–51. [PubMed: 15908146]
- [60]. Beugnet A, Tee AR, Taylor PM, Proud CG. Regulation of targets of mTOR (mammalian target of rapamycin) signalling by intracellular amino acid availability. *Biochem. J* 2003;372:555–66. [PubMed: 12611592]
- [61]. Tremblay F, Marette A. Amino acid and insulin signaling via the mTOR/p70 S6 kinase pathway. A negative feedback mechanism leading to insulin resistance in skeletal muscle cells. *J. Biol. Chem* 2001;276:38052–60. [PubMed: 11498541]
- [62]. Khamzina L, Veilleux A, Bergeron S, Marette A. Increased activation of the mammalian target of rapamycin pathway in liver and skeletal muscle of obese rats: possible involvement in obesity-linked insulin resistance. *Endocrinology* 2005;146:1473–81. [PubMed: 15604215]
- [63]. Cunningham JT, Rodgers JT, Arlow DH, Vazquez F, Mootha VK, Puigserver P. mTOR controls mitochondrial oxidative function through a YY1-PGC-1 α transcriptional complex. *Nature* 2007;450:736–40. [PubMed: 18046414]
- [64]. Katz A. Modulation of glucose transport in skeletal muscle by reactive oxygen species. *J. Appl. Physiol* 2007;102:1671–6. [PubMed: 17082366]
- [65]. Yakes FM, Van Houten B. Mitochondrial DNA damage is more extensive and persists longer than nuclear DNA damage in human cells following oxidative stress. *Proc. Natl. Acad. Sci. U. S. A* 1997;94:514–9. [PubMed: 9012815]
- [66]. Dawson TL, Gores GJ, Nieminen AL, Herman B, Lemasters JJ. Mitochondria as a source of reactive oxygen species during reductive stress in rat hepatocytes. *Am. J. Physiol* 1993;264:C961–7. [PubMed: 8386454]
- [67]. Chabi B, Ljubicic V, Menzies KJ, Huang JH, Saleem A, Hood DA. Mitochondrial function and apoptotic susceptibility in aging skeletal muscle. *Aging Cell*. 2007
- [68]. Crompton M. The mitochondrial permeability transition pore and its role in cell death. *Biochem. J* 1999;341(Pt 2):233–49. [PubMed: 10393078]
- [69]. Tonkonogi M, Walsh B, Svensson M, Sahlin K. Mitochondrial function and antioxidative defence in human muscle: effects of endurance training and oxidative stress. *J Physiol* 2000;528(Pt 2):379–88. [PubMed: 11034627]
- [70]. Wiley SE, Murphy AN, Ross SA, van der Geer P, Dixon JE. MitoNEET is an iron-containing outer mitochondrial membrane protein that regulates oxidative capacity. *Proc. Natl. Acad. Sci. U. S. A* 2007;104:5318–23. [PubMed: 17376863]
- [71]. Paddock ML, Wiley SE, Axelrod HL, Cohen AE, Roy M, Abresch EC, Capraro D, Murphy AN, Nechushtai R, Dixon JE, Jennings PA. MitoNEET is a uniquely folded 2Fe 2S outer mitochondrial membrane protein stabilized by pioglitazone. *Proc. Natl. Acad. Sci. U. S. A* 2007;104:14342–7. [PubMed: 17766440]

- [72]. Michishita E, Park JY, Burneskis JM, Barrett JC, Horikawa I. Evolutionarily conserved and nonconserved cellular localizations and functions of human SIRT proteins. *Mol. Biol. Cell* 2005;16:4623–35. [PubMed: 16079181]
- [73]. Xie J, Marusich MF, Souda P, Whitelegge J, Capaldi RA. The mitochondrial inner membrane protein mitofilin exists as a complex with SAM50, metaxins 1 and 2, coiled-coil-helix coiled-coil-helix domain-containing protein 3 and 6 and DnaJC11. *FEBS Lett* 2007;581:3545–9. [PubMed: 17624330]
- [74]. Kim JY, Tillison KS, Zhou S, Lee JH, Smas CM. Differentiation-dependent expression of Adhfe1 in adipogenesis. *Arch. Biochem. Biophys* 2007;464:100–11. [PubMed: 17559793]
- [75]. Belyaeva OV, Korkina OV, Stetsenko AV, Kedishvili NY. Human retinol dehydrogenase 13 (RDH13) is a mitochondrial short-chain dehydrogenase/reductase with a retinaldehyde reductase activity. *Febs J* 2007;275:138–47. [PubMed: 18039331]
- [76]. Fukada K, Zhang F, Vien A, Cashman NR, Zhu H. Mitochondrial proteomic analysis of a cell line model of familial amyotrophic lateral sclerosis. *Mol Cell Proteomics* 2004;3:1211–23. [PubMed: 15501831]
- [77]. Calvo S, Jain M, Xie X, Sheth SA, Chang B, Goldberger OA, Spinazzola A, Zeviani M, Carr SA, Mootha VK. Systematic identification of human mitochondrial disease genes through integrative genomics. *Nat. Genet* 2006;38:576–82. [PubMed: 16582907]
- [78]. Hajek P, Chomyn A, Attardi G. Identification of a novel mitochondrial complex containing mitofusin 2 and stomatin-like protein 2. *J. Biol. Chem* 2007;282:5670–81. [PubMed: 17121834]
- [79]. Mootha VK, Bunkenborg J, Olsen JV, Hjerrild M, Wisniewski JR, Stahl E, Bolouri MS, Ray HN, Sihag S, Kamal M, Patterson N, Lander ES, Mann M. Integrated analysis of protein composition, tissue diversity, and gene regulation in mouse mitochondria. *Cell* 2003;115:629–40. [PubMed: 14651853]

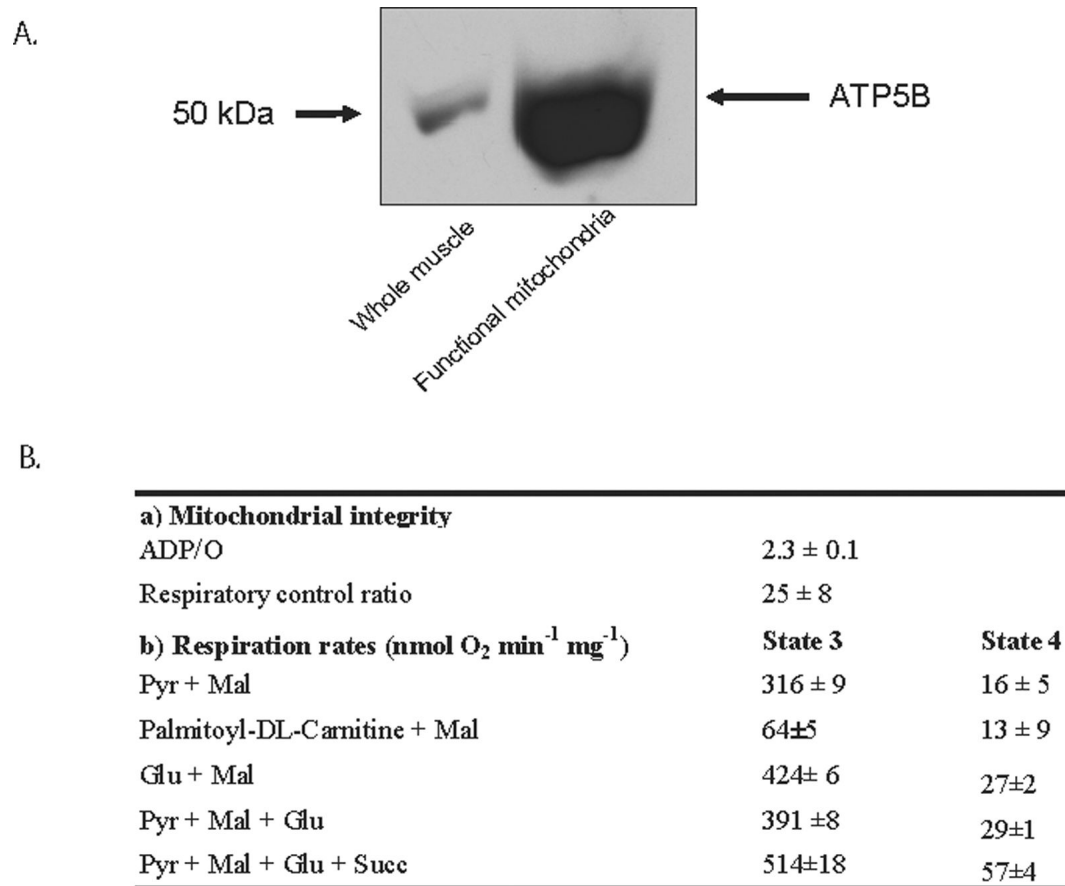


Figure 1. Mitochondria enrichment and functional assessment

(A) Western blot showing the increase in ATP synthase (beta subunit) in the mitochondria-enriched fraction compared to equal amount of whole muscle lysate. (B) Isolated mitochondria response to maximal concentrations of substrates in the presence of 0.5 mM ADP (State 3 respiration) and in the absence of ADP (State 4 respiration). ADP/O ratio and RCR were calculated using Pyr + Mal data.

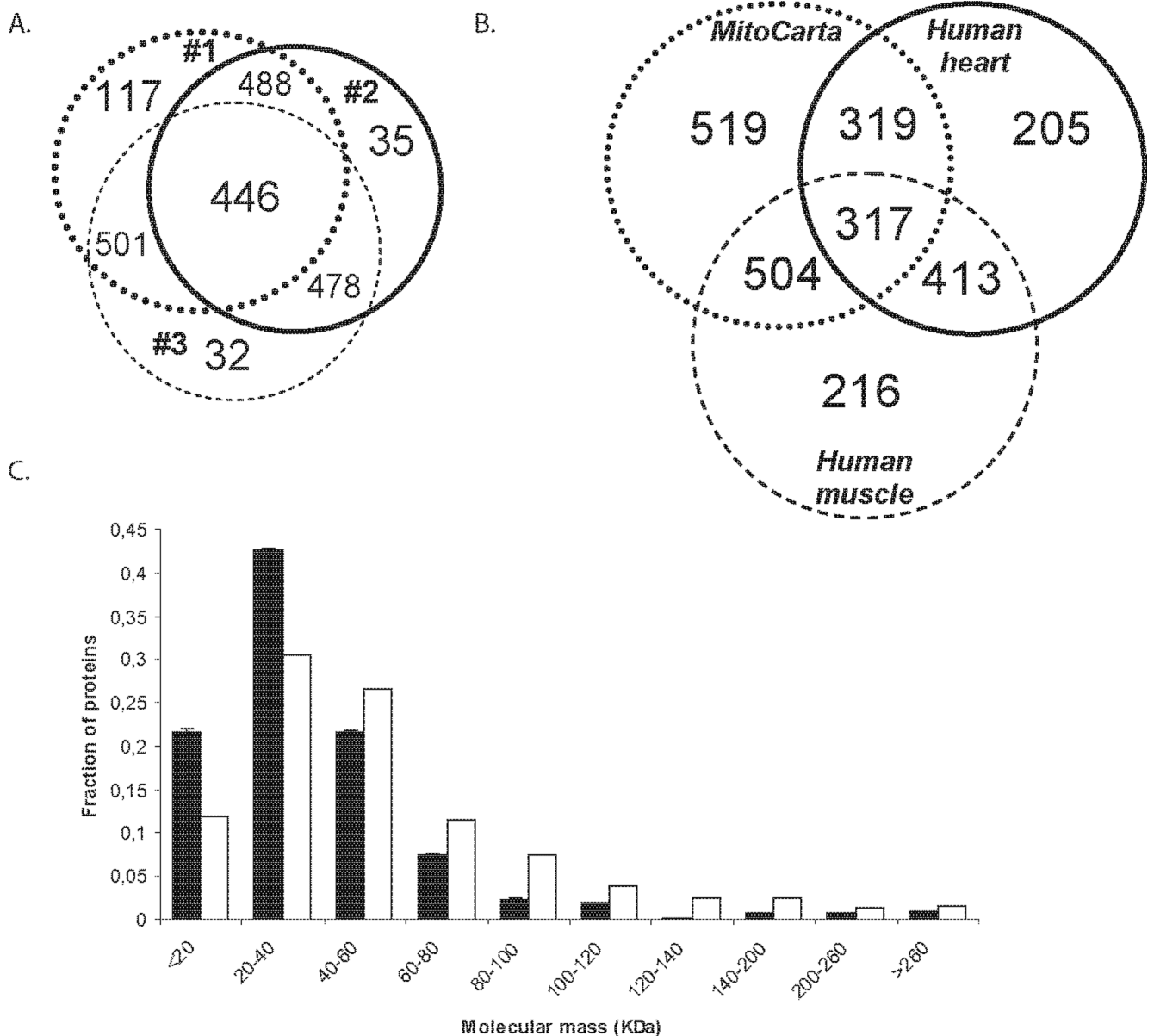


Figure 2. Skeletal muscle mitochondria database comparison and molecular mass distribution
 (A) Venn diagram showing the number of common unique proteins found in two or all mitochondrial fractions from subjects #1-3. (B) Diagram showing the number of proteins shared between the present study and previously published mitochondrial proteomes from mouse [20] and human heart [7,23]. (C) Molecular mass distribution of the 823 detected proteins on the isolated mitochondrial fractions (n=3) (■) by HPLC-ESI-MS/MS compared to the 954 proteins in the whole muscle proteome (□) dataset [43].

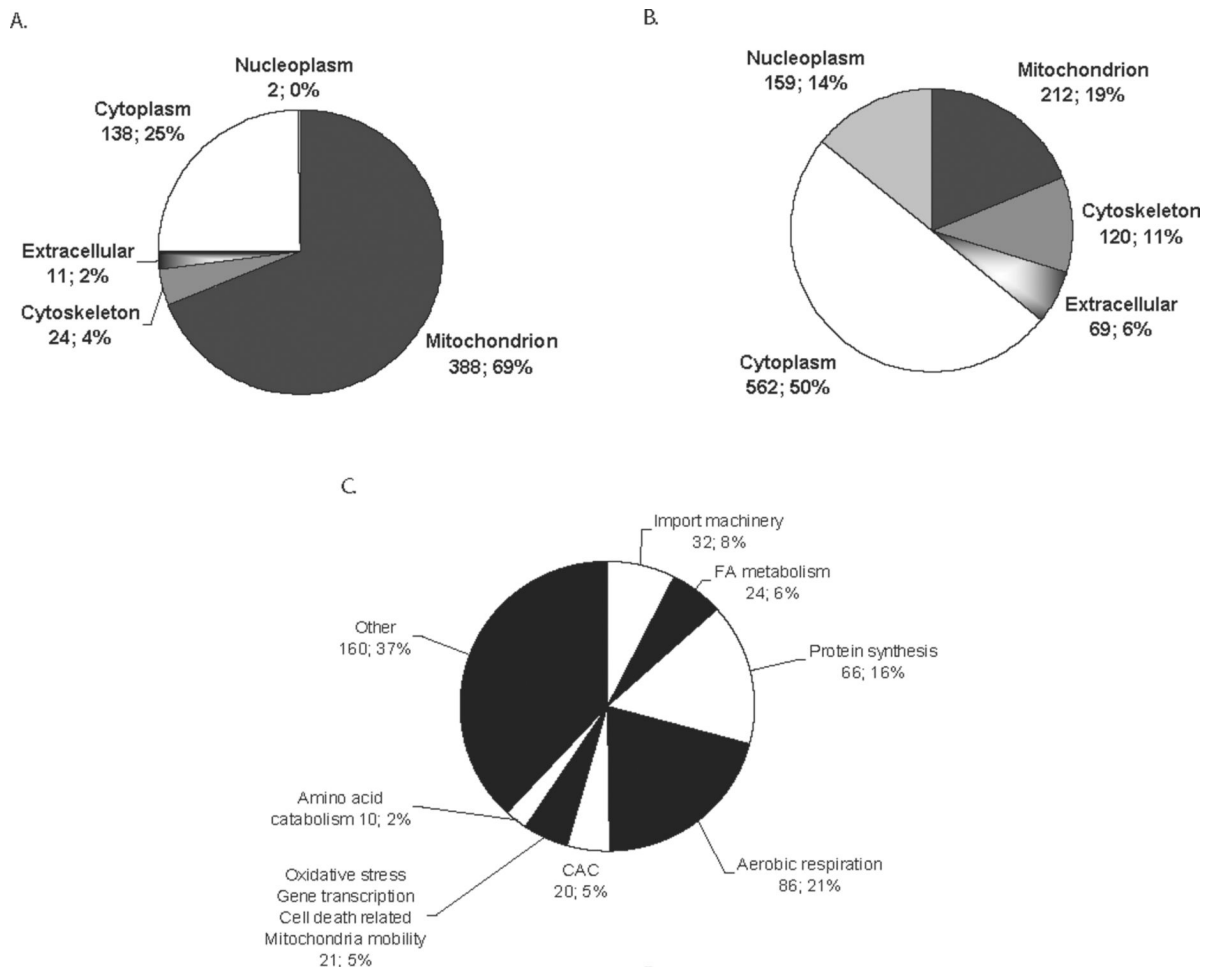


Figure 3. Cellular location and biological function of proteins detected in the human skeletal muscle mitochondria enriched fraction

(A) Cellular compartment distribution of the proteins detected in the mitochondrial proteome (60 μ g and the single 240 μ g loads were pooled for this analysis) and whole muscle proteome (B) [43] according to Gene Ontology information. (C) Only proteins annotated to mitochondria according to GO (388 proteins) were included in this analysis. Function of the mitochondria-specific proteins detected in the mitochondrial proteome. The cellular compartment/function is followed by the number of proteins and the % of proteins assigned.

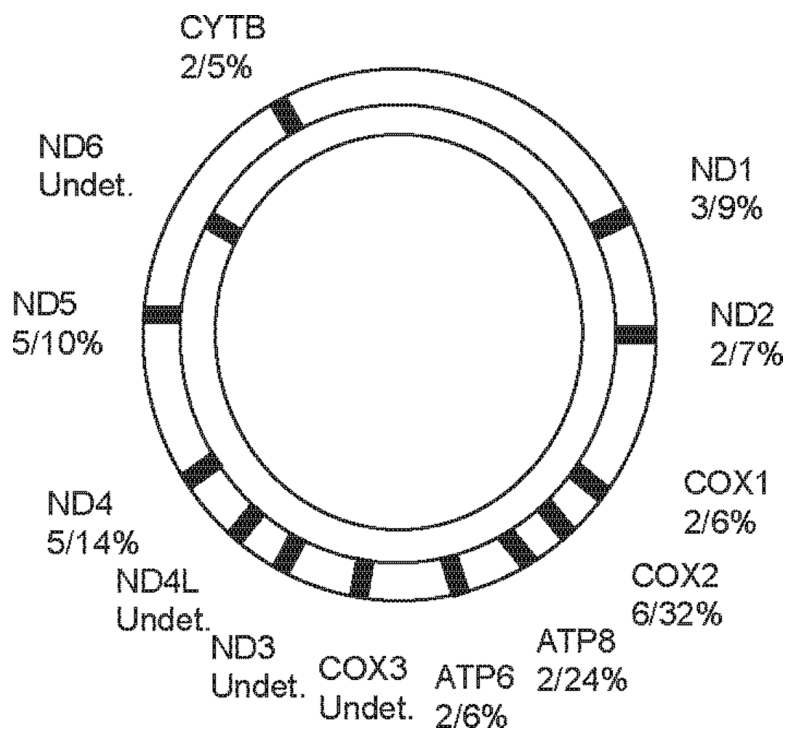


Figure 4. Detection of mitochondrial DNA-encoded proteins in human skeletal muscle mitochondria

Number of unique peptides and sequence coverage (# unique peptides/% sequence coverage) of the 13 mitochondrial DNA-encoded proteins detected by HPLC-ESI-MS/MS in the mitochondrial fraction. The 22 tRNAs have been omitted from the mtDNA genome heavy chain (coding for all subunits except ND6) and the light chain for simplicity.

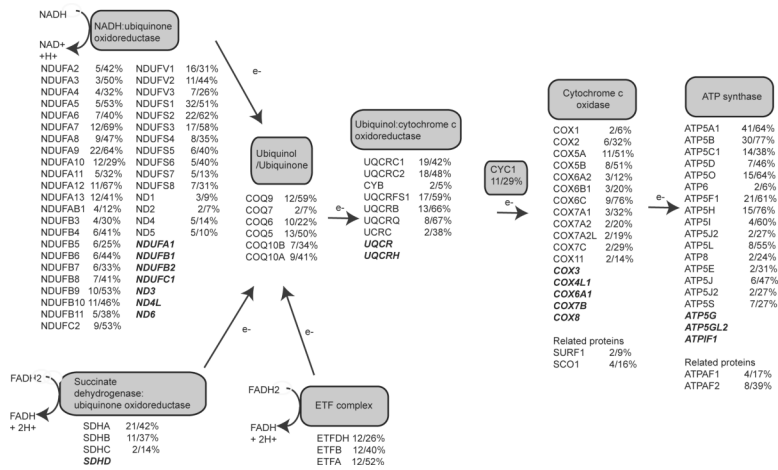


Figure 5. Detection of electron transport chain and oxidative phosphorylation subunits and related proteins

If the subunit is ***bold and italic***, it is absent from the dataset. The gene names are followed by the #unique peptides/ % sequence coverage. Gene names listed under ubiquinone are involved in the biosynthesis of the coenzyme.

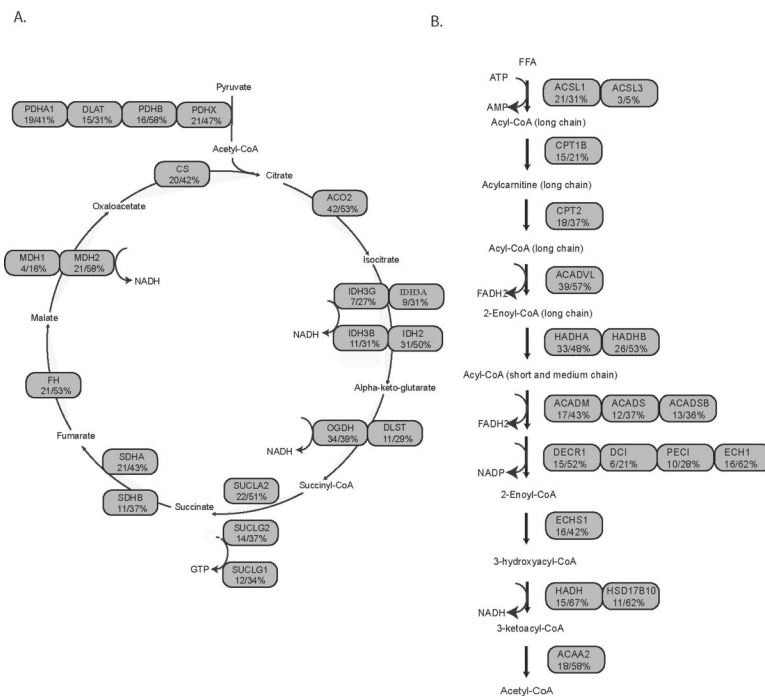


Figure 6. CAC and fatty acid oxidation proteins detected in human skeletal muscle isolated mitochondria

Detection of proteins in the citric acid cycle (A) and in the fatty acid oxidation pathway (B). Gene names are followed #unique peptides/ % sequence coverage.

Table 1

(A) Proteins detected in human skeletal muscle mitochondria not currently annotated to mitochondria according to Gene Ontology and presenting literature (www.pubmed.org) evidence of mitochondrial localization. (B) Proteins detected in human skeletal muscle mitochondria with undefined cellular localization.

Protein	Gene name	Molecular Mass (kDa)	Max. unique peptides	Max. sequence coverage (%)	Ref
Evidence of mitochondrial localization					
<i>Newly characterized</i>					
Iron containing alcohol dehydrogenase 1	ADHFE1	50	10	32	[74]
ADP-ribosylation factor-like protein 2	ARL2	21	5	30	[52]
ATPase family AAA domain-containing protein 3A	ATAD3A	71	12	30	[47,75]
Retinol dehydrogenase 13	RDH13	36	10	34	[75]
NAD-dependent deacetylase sirtuin-5 1/2	SIRT5	34	5	22	[72]
Zinc finger, CDGSH-type domain	CISD2	15	3	21	[70]
<i>Uncharacterized</i>					
Uncharacterized protein KIAA0152 precursor	KIAA0152	32	4	21	[76]
Transmembrane protein 70	TMEM70	29	4	20	[77]
Stomatin-like protein 2	STOML2	39	11	38	[78]
Protein NipSnap3A	NIPSNAP3A	28	9	50	[79]
ERV1-like growth factor	GFER	23	2	13	[79]
Similar to nucleoside diphosphate-linked moiety X motif 19	NUDT19	50	3	8	[79]
Up-regulated during skeletal muscle growth protein 5	USMG5	7	5	47	[19,79]
B.					
<i>Unknown cellular location</i>					
Isoform 1/2 of cat eye syndrome critical region protein 5 precursor	CECR5	45	8	28	
Coiled-coil domain-containing protein 127	CCDC58	17	5	39	
Isoform A of uncharacterized protein C20ORF108	C20orf108	20	2	15	
Thioredoxin domain-containing protein 13 precursor	TXNDC13	39	4	11	
Isoform 1/2/3 of uncharacterized protein C6ORF136	C6orf136	26	4	10	
Isoform 1/4 of abhydrolase domain-containing protein 11	ABHD11	34	9	45	
Isoform 2 of Bcl10-interacting card protein kinase type-2 B	C9orf89	21	6	29	
Isoform 1/2 of phosphatidylinositol-4-phosphate 4-kinase type-2 B	PIP4K2B	40	4	13	
Core histone macro-H2A	H2AFY2	40	3	10	
Uncharacterized protein C18ORF19	C18orf19	31	2	3	
Uncharacterized protein C2ORF47	C2orf47	33	5	21	
Uncharacterized protein C9ORF46	C9orf46	17	5	27	
Carbonic reductase	CBR4	25	6	32	
Uncharacterized protein C3ORF60	C3orf60	20	5	38	
15 kDa protein	C3orf60	15	5	31	
Protein Fam82B	FAM82B	48	8	22	
Hypothetical protein LOC347273	LOC347273	42	2	6	
Uncharacterized protein C10ORF58	C10orf58	25	7	31	
Isoform 2 of UPF0105 protein C14ORF124	C14orf124	31	6	29	
Methyltransferase-like protein 7A precursor	METTL7A	28	4	20	
Isoform 1/2 of coiled-coil domain containing protein 109A	CCDC109A	38	12	29	
Protein NipSnap3B	NIPSNAP3B	28	12	53	
Fun14 domain containing 2	FUNDC2	22	5	25	
Hypothetical protein LOC125988	P117	13	3	41	
E2-induced gene 5 protein	C3orf28	17	7	32	

A.

Protein	Gene name	Molecular Mass (kDa)	Max. unique peptides	Max. sequence coverage (%)	Ref
165 kDa protein		165	56	47	
Acylphosphatase, muscle type isozyme	ACYP2	13	5	44	
Coiled-coil domain-containing protein 127	CCDC127	31	2	10	
Uncharacterized protein C19ORF52	C19orf52	29	3	15	
Hypothetical protein LOC112812 isoform 1	FDX1L	20	2	15	
Lyr motif-containing protein 5	LYRM5	11	4	30	
Isoform 1 of UPF0366 protein C11ORF67	C11orf67	13	2	22	
Hypothetical protein LOC23078 isoform A	K0564	215	2	1	
Hypothetical protein LOC137682	C8orf38	38	4	16	
PTC7 protein phosphatase homolog	PPTC7	33	2	10	
Lyr motif-containing protein 7	LYRM7	12	2	24	
Hypothetical protein LOC55471 isoform 1	C2orf56	49	2	5	
Hypothetical protein MGC3196	MGC3196	22	3	22	
Conserved hypothetical protein	C6orf203	28	4	24	
Guanine nucleotide-binding protein subunit beta 2	GNB1/2	25	2	6	
Histidine triad nucleotide-binding protein 3	HINT3	20	2	14	
FLJ10769 protein	FLJ10769	39	4	16	
Uncharacterized protein C22ORF32	C22orf32	11	2	26	

Table 2

Subsets of mitochondrial proteins detected in the mitochondria proteome.

Protein	Gene name	Molecular Mass (kDa)	Max. unique peptides	Max. seq. coverage (%)
Import machinery and transporters				
ADP/ATP translocase 1	SLC25A4	33	4	17
ADP/ATP translocase 2	SLC25A5	33	16	44
ADP/ATP translocase 3	SLC25A6	33	3	10
AFG3-like protein 2	AFG3L2	88	15	24
ATP-binding cassette sub-family B member 10	ABCB10	79	2	4
Calcium-binding mitochondrial carrier protein Aralar1	SLC25A12	75	35	56
Carnitine O-palmitoyltransferase 2	CPT2	74	18	37
Carnitine O-palmitoyltransferase I	CPT1B	88	15	21
GrpE protein homolog 1	GRPEL1	24	5	29
Import inner membrane translocase subunit TIM44	TIMM44	51	8	20
Import inner membrane translocase subunit TIM50	TIMM50	40	6	18
Leucine zipper-EF-hand-containing transmembrane protein 1	LETM1	83	5	8
Metaxin-1	MTX1	36	5	15
Metaxin-2	MTX2	30	9	34
Mitochondrial 2-oxoglutarate/malate carrier protein	SLC25A11	34	17	61
Mitochondrial carnitine/acylcarnitine carrier protein	MCAT	33	2	6
Mitochondrial carrier homolog 1 (Presenilin-associated protein)	MTCH1	42	2	5
Mitochondrial carrier homolog 2 (Met-induced mito protein)	MTCH2	33	7	27
Import inner membrane translocase subunit TIM9	TIMM9	10	2	26
Mitochondrial import inner membrane translocase subunit Tim13	TIMM13	11	3	37
Mitochondrial import inner membrane translocase subunit Tim17-B	TIMM17B	18	3	30
Mitochondrial import inner membrane translocase subunit Tim23	TIMM23	22	4	26
Mitochondrial import receptor subunit TOM22 homolog	TOMM22	15	6	63
Mitochondrial intermembrane space import and assembly protein 40	CHCHD4	16	3	26
Mitochondrial-processing peptidase alpha subunit	PMPCA	58	7	17
Mitochondrial-processing peptidase subunit beta	PMPCB	54	5	14
Phosphate carrier protein, mitochondrial precursor	SLC25A3	40	17	34
Probable mitochondrial import receptor subunit TOM40 homolog	TOMM40	38	5	20
Voltage-dependent anion-selective channel protein 1	VDAC1	31	19	73
Voltage-dependent anion-selective channel protein 2	VDAC2	38	11	40
Voltage-dependent anion-selective channel protein 3	VDAC3	31	13	48
Protein synthesis				
Elongation factor Ts	TSEFM	35	7	27
Elongation factor Tu	TUFM	50	20	51
Isoleucyl-tRNA synthetase	IARS2	114	9	12
Probable glutamyl-tRNA synthetase	EARS2	59	2	4
Seryl-tRNA synthetase	SARS2	58	7	22
Tyrosyl-tRNA synthetase	YARS2	53	3	8
Histidyl-tRNA synthetase	HARS2	57	3	7
Dihydroorotate dehydrogenase	DHODH	43	7	26
Transcription factor A	TFAM	29	10	38
Oxidative stress proteins				
Glutathione S-transferase kappa 1	GSTK1	25	9	55
Peroxisredoxin-5	PRDX5	22	7	37
Phospholipid hydroperoxide glutathione peroxidase	GPX4	22	5	29
Superoxide dismutase (Mn)	SOD2	25	16	68
Thioredoxin reductase 2	TXNRD2	56	3	7
Unfolding protein response				
10 heat shock protein	HSPE1	11	8	63
60 heat shock protein	HSPD1	61	36	65
Heat shock protein 75	TRAP1	80	14	27
Serine protease HTRA2	HTRA2	49	7	22
Stress-70 protein	HSPA9	74	27	44
Kinases and phosphatases				
Adenylate kinase isoenzyme 2	AK2	26	9	48
Creatine kinase	CKMT2	48	19	41
GTP:AMP phosphotransferase mitochondrial	AK3	25	16	75
Inorganic pyrophosphatase 2	PPA2	38	7	29
Protein-tyrosine phosphatase mitochondrial 1	PTPMT1	23	6	41
Cell death related proteins				
Bcl-2 homologous antagonist/killer	BAK1	23	5	42
DnaJ homolog subfamily A member 3	DNAJA3	53	6	15

Protein	Gene name	Molecular Mass (kDa)	Max. unique peptides	Max. seq. coverage (%)
Programmed cell death protein 8	AIFM1	67	22	43
Diablo homolog	DIABLO	27	8	26
Chaperone-activity of bc1 complex-like	CABC1	72	18	32
Endonuclease G	ENDOG	33	7	35
Grim 19	NDUFA13	26	12	41
<i>Amino acid catabolism</i>				
Branched chain aminotransferase 2	BCAT2	44	10	33
2-oxoisovalerate dehydrogenase alpha subunit	BCKDHA	50	6	23
Lipoamide acyltransferase	DBT	53	9	26
Alpha-ketoglutarate dehydrogenase	OGDH	116	34	39
Aspartate aminotransferase	GOT2	47	26	57
Delta-1-pyrroline-5-carboxylate dehydrogenase	ALDH4A1	62	23	48
Glutamate dehydrogenase	GLUD1	61	14	29
Glutaryl-CoA dehydrogenase	GCDH	48	2	8
Glycine cleavage system H protein	GCSH	19	2	17
Hydroxymethylglutaryl-CoA lyase	HMGCL	34	4	19
Isovaleryl-CoA dehydrogenase	IVD	46	13	42
Methylmalonate semialdehyde dehydrogenase	ALDH6A1	58	13	26
Methylcrotonyl-CoA carboxylase alpha	MCCC1	81	5	12
Methylcrotonyl-CoA carboxylase beta	MCCC2	61	11	25
<i>Iron related proteins</i>				
HESB-like domain-containing protein 2	ISCA1	14	2	22
Fratxin, mitochondrial precursor	FXN	23	4	20
Ferrochelatase	FECH	48	5	22
Coproporphyrinogen III oxidase	CPOX	50	5	13